Disilane Internal Rotation

Vojislava Pophristic, Lionel Goodman,* and Cheryl T. Wu

Wright and Rieman Chemistry Laboratories, Rutgers, The State University of New Jersey, New Brunswick, New Jersey 08903

Received: April 10, 2001; In Final Form: June 5, 2001

Energetics of hindered rotation in disilane are analyzed and compared to ethane. In disilane weakened (rotationally governed) hyperconjugative interactions, paramount in controlling the ethane barrier, leave the nonrotational part of the torsional coordinate as the primary contribution to disilane barrier energetics. In this regard, the 0.012 Å Si−Si bond lengthening that accompanies rotation is found to account for most of the 1.0 kcal/mol barrier. Although both the Si−Si bond expansion in disilane and the 0.014 Å C−C bond expansion in ethane are nearly the same, the mechanisms for these expansions are found to be different. Unlike in ethane, where the expansion is largely due to the hyperconjugation decrease in the eclipsed conformer, in disilane it is almost entirely due to electrostatic repulsion between Si−H bonds in the two silyl groups.

I. Introduction

Theoretical studies during the past decade[1−3] raised questions about the validity of the steric repulsion model,[4,5] rationalizing ethane's torsional barrier. The major thrust of the early work on the origin of the torsional barrier lies in the change in exchange (overlap) repulsion between C−H bonds of the two respective methyl groups (Figure 1a).[4,6] This chemically appealing view became popular and is dominantly in use in the chemical community.

The issue of the relative contribution of other effects has been considered extensively over the years. The first study contradicting the exchange repulsion idea was that of Brunck and Weinhold in 1979.[7] These authors, building on work of England and Gordon,[8] ascribed the origin of the ethane barrier to preferential hyperconjugative stabilization of the staggered (*S*) conformer. A more recent barrier origin consideration is central C−C bond weakening.[2] The current position is that both the staggered conformational preference and the barrier stem from the hyperconjugative interactions.[1,7,9,10] In coming to a conclusive decision on the internal rotation mechanism it is necessary to include the full coordinate space of the ethane torsion. Internal rotation is not pure rotation. In the case of ethane, the torsional coordinate includes C−C bond expansion. If this lengthening is disregarded, then the hyperconjugative origin for the barrier is not validated.[10]

Because both hyperconjugation and steric repulsion strongly depend on the relative position of the two rotors, disilane represents an interesting extension of the ethane barrier problem. It can be thought of as stretched ethane (the central bond is 0.84 Å longer than in ethane) enriched by additional electrons. Disilane is also important in its own right as the simplest example involving internal rotation of the SiH_3 group. Although electron diffraction experiments do not establish whether the equilibrium conformation is staggered (*S*) or eclipsed (*E*) (because H atoms contribute little to the diffraction pattern),[11] all reported calculations[12] find, as in ethane, that the lowest energy (equilibrium) state is staggered (Figure 1). Both sources conclude longer Si−H bonds, and a somewhat larger HSiH angle than the corresponding ones in ethane (Table 1). Rotating one silyl group by 60° then produces an eclipsed, higher energy conformation (Figure 1b). The barrier to this process has been both calculated by a variety of methods and experimentally determined from gas-phase Raman frequencies to be near 1 kcal/mol (experiment: 1.26 kcal/mol;[13] theory: 0.82−1.09 kcal/mol[12,14−19]).

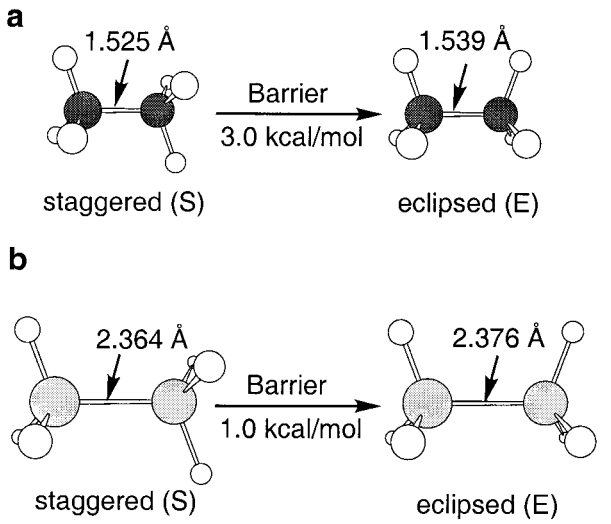

Figure 1. Internal rotation in ethane (a) and disilane (b), showing equilibrium (staggered, *S*) and top-of-barrier (eclipsed, *E*) conformers.

Although there are a number of publications establishing the torsional barrier in disilane, only a few attempt to ascribe its origin.[20,21] In 1992 Schleyer and co-workers[15] gave a detailed account of the disilane torsional barrier origin, working within the hyperconjugation model, using a 3-21G(d,p) ab initio basis set. They found that the change in hyperconjugative interactions on going to the eclipsed conformer (calculated as 0.9 kcal/mol) approximated their calculated barrier (0.82 kcal/mol), suggesting that these interactions should be taken as responsible for the existence of the barrier. However, no account of other changes, such as bond strengthenings or weakenings, or exchange repulsion was taken.

* Corresponding author.

10.1021/jp011326c CCC: $20.00
Published on Web 07/17/2001

TABLE 1: HF/6-311G(3df,2p) Optimized Geometries of Disilane and Ethane (bond lengths in Å, bond angles in degrees)

	disilane		ethane	
internal coordinate	*S* conformer	*E* conformer	*S* conformer	*E* conformer
Si−Si, C−C bond length	2.364	2.376	1.525	1.539
Si−H, C−H bond length	1.478	1.478	1.084	1.083
∠HSiH, ∠HCH	108.6	108.5	107.7	107.2

Our aim is to reanalyze disilane internal rotation, considering the interplay of the major factors that are now recognized to play a major role in torsional phenomena, i.e., bond strength, hyperconjugation, and repulsion changes,[3] at a sufficiently high level of theory to give physically meaningful conclusions. In particular, account must be taken of the nonrotational part of the coordinate space of disilane internal rotation (which as in ethane includes central bond lengthening). By comparing the results with the hyperconjugation model for ethane torsion, we pose the question: do the gears and motors that control the ethane barrier operate in the same way in disilane?

II. Calculational Schemes

To separate the structural enlargement and the electron enrichment factors, two schemes are considered involving the "phantom molecules", $(ET)_{DS}$ and $(DS)_{ET}$:

$$\text{I}\quad \text{ETHANE} \xrightarrow{\textit{structural enlargement}} (ET)_{DS} \xrightarrow{\textit{electron enrichment}} \text{DISILANE}$$

$$\text{II}\quad \text{ETHANE} \xrightarrow{\textit{electron enrichment}} (DS)_{ET} \xrightarrow{\textit{structural enlargement}} \text{DISILANE}$$

Scheme I takes ethane to the more open molecular structure of disilane without any electronic configuration change, $(ET)_{DS}$. Addition of the third row electrons then yields disilane. In Scheme II the ethane molecular structure is frozen, but with an electron configuration appropriate to disilane, $(DS)_{ET}$. The second step in this scheme, expansion of the molecular structure, gives disilane. The abbreviation in the parenthesis (e.g., (ET)) represents the electronic configuration of the phantom molecule, whereas the subscript corresponds to the phantom molecule geometry.

III. Disilane Rotational Barrier

Fully relaxed internal rotation (FR) is defined by rotating one dihedral angle of a silyl group (the "rotational angle") and optimizing all other structural parameters. The energy required to rotate the *S* conformer to the *E* conformer

$$\Delta E_B(\text{FR}) = E^E(\text{FR}) - E^S \tag{1a}$$

is the fully relaxed rotation geometry barrier, analogous to ethane. HF/6-311G(3df,2p) optimized geometries for both *S* and *E* conformers are reported in Table 1. Internal coordinate values of the *S* and *E* conformers essentially agree with those found in extensive studies by Leszczynski et al.[22] and others,[12] as well as with the experimental ones.[11] The 1.0 kcal/mol barrier is also consistent with previous studies.[12,14−19] This value is ∼1/3 ethane's 3.0 kcal/mol barrier and this difference does not provide, by itself, any discrimination between the various interactions postulated to rationalize the ethane barrier. In fact, the large barrier decrease in going from ethane to disilane is simplistically in agreement with both distance attenuated pairwise repulsions and vicinal hyperconjugative interactions between Si−H bonds (of the two methyl/silyl groups).

TABLE 2: Rigid Rotation and Fully Relaxed Barriers for Disilane, Ethane, and Phantom Molecules, $(ET)_{DS}$ and $(DS)_{ET}$, (kcal/mol)[a,b]

	ΔE_B(RR)	ΔE_B(FR)
disilane	1.06	1.03
ethane	3.17	3.03
$(ET)_{DS}$[b]	0.28	1.38
$(DS)_{ET}$[b]	10.84	−2.84

[a] HF/6-311G(3df,2p) geometries and energy calculations. Rounded off to the nearest 0.01 kcal/mol, as is the case with all other energy values reported in this work. [b] For notation, see Section II.

The rigid rotation (RR) barrier (i.e., rotation proceeds without relaxation of bond lengths or bond angles) is

$$\Delta E_B(\text{RR}) = E^E(\text{RR}) - E^S \tag{1b}$$

As demonstrated in Table 2, the rigid rotation barriers for both ethane and disilane are only slightly different from the fully relaxed ones, showing that no severe error in the barrier energy is imposed by this model. This near equality obscures the physics underlying the internal rotation barriers in these molecules.

Since the level of theory has little effect on the calculated barrier energy, the polarization saturated Hartree−Fock wave function, HF/6-311G(3df,2p), is adopted (unless noted) for the barrier analysis reported in this article. Energy calculations and geometry optimizations were performed using Gaussian 98,[23] and natural bond orbital analysis utilized NBO 4.M.[24]

IV. Phantom Molecule Barriers

The phantom molecule, $(ET)_{DS}$ and $(DS)_{ET}$, rotation barriers provide a clear delineation between the expansion and electron enrichment factors. For the expanded ethane structure $(ET)_{DS}$ the calculated RR barrier almost vanishes (Table 2), but the electron enriched $(DS)_{ET}$ ethane-structure barrier is found to be strongly increased. The fully relaxed barrier for $(ET)_{DS}$ also significantly decreases from that in ethane, but the $(DS)_{ET}$ barrier is negative. It is noteworthy that the negative value, $\Delta E_B(\text{FR}) < 0$ for $(DS)_{ET}$ indicates that the preferred equilibrium conformer has changed to the eclipsed one.

In the "extended" ethane, $(ET)_{DS}$, the primary barrier forming process is not rotation, but central bond lengthening, since the RR barrier almost vanishes. On the other hand, just rotating silyl groups in $(DS)_{ET}$ strongly destabilizes the *E* conformer—it is the central bond lengthening that relieves the strain accumulated by rotation and turns around the conformational preference.

The fully relaxed entries in Table 2 demonstrate that the barrier attenuation in going from ethane to disilane is a combined effect of structural expansion and electron enrichment: each of these factors decreases the ethane barrier. The result that structural expansion is a cause for the ethane → disilane barrier attenuation is not unexpected. However, the question remains: which structural expansion represents the smoking gun for the barrier attenuation? These expansions, as revealed in Table 1, are the following: increase of the equilibrium conformer central atom bond length from 1.53 to 2.36 Å in disilane, and opening up of the CH_3 umbrella to the more tetrahedral SiH_3 structure, comprising an ∠HCH increase from 107.7° to 108.6° for ∠HSiH and lengthening of the C−H bond from 1.08 to 1.48 Å for Si−H.

This question can be conclusively answered by examining the calculated barriers for the two partial structural expansions in going from ethane → $(ET)_{DS}$, shown in Table 3. The barrier

TABLE 3: Calculated Barriers for Partial Structural Expansions Taking Ethane to $(ET)_{DS}$ (kcal/mol)[a,b]

model	ΔE_B
ethane	3.03
$(ET)_{SiH_3}$	5.63
$(ET)_{SiSi}$	1.33
$(ET)_{DS}$	1.38
disilane	1.03

[a] Partial relaxations simulate fully relaxed behavior of the particular disilane internal coordinate (e.g., Si−Si bond length), whereas the other internal coordinates (except rotational angle) assume ethane equilibrium values. [b] See Table 2, footnotes *a* and *b*. See Section IV.

TABLE 4: Fully Relaxed Barrier Decompositions (kcal/mol)[a,b]

model	ΔE_B	ΔE_{struct}	$\Delta E_{exchange}$	ΔE_{deloc}
ethane	3.03	2.17	−5.75	6.61
disilane	1.03	2.95	−2.60	0.68
$(ET)_{DS}$	1.38	2.03	−0.63	−0.02

[a] See Section V, and Table 2, footnotes *a* and *b*. [b] Total barrier energy is the sum of structural, exchange and delocalization energy changes.

energy $\Delta E_B(ET)_{SiSi}$ represents the partially rigid rotation barrier computed for ethane with central bond lengthening as in disilane (i.e., the phantom C−C bond lengthens from 2.36 to 2.38 Å) along with rigid rotation (the other structural alteration absent). Similarly, $\Delta E_B(ET)_{SiH_3}$ represents the barrier for SiH_3 flexing present along with rigid rotation (central bond length fixed at ethane's 1.525 Å). Comparison of the $(ET)_{SiSi}$ and ethane entries shows that the barrier attenuation arises from expansion of the central atom bond length, alone. In contrast, the barrier for $(ET)_{SiH_3}$ (involving only SiH_3 flexing) is increased. Combining this result with the vanishing rigid rotation barrier for $(ET)_{DS}$ (rotation occurring at C−C length of 2.36 Å, with no rotationally induced relaxation, Table 2) shows that it is the central bond expansion in going from ethane to disilane that attenuates the barrier.

V. Barrier Mechanism

(a) General Considerations. At first consideration it appears that the same barrier mechanism machinery that operates in ethane rationalizes the attenuation of the barrier in going from ethane to disilane. That is, the central bond expansion reduces the hyperconjugative interactions between the silyl groups from those between the methyl groups in ethane. We turn to natural bond orbital (NBO) theory[25] to provide an incisive means for examining the mechanisms controlling barrier energetics in more detail. The NBO approach allows a natural dissection[26] of the barrier energy into hyperconjugative (ΔE_{deloc}), exchange ($\Delta E_{exchange}$) and structural (ΔE_{struct}) energy contributions. In this formulation, the hyperconjugative donor−acceptor (i.e., charge-transfer or delocalization) interactions, E_{deloc}, can be readily assessed by deleting (minimally occupied) antibonding orbitals.[27] The Pauli-exchange effect,[28] $E_{exchange}$, is the energy difference between orthogonal (NBO) and nonorthogonal (preNBO, PNBO) wave function descriptions of the molecule.[29] The effect of bond weakenings and strengthenings accompanying the rotation, i.e., the sense of the structural energy change, ΔE_{struct}, incorporating the main localized bonds of the "Lewis" structure, can be assessed from changes in NBO energies. However, because bond strengths involve more than orbital effects, this procedure is not very quantitative and we estimate ΔE_{struct} as the residual in $\Delta E_B - (\Delta E_{exchange} + \Delta E_{deloc})$.

Table 4 gives the energy changes, ΔE_{struct}, $\Delta E_{exchange}$, and ΔE_{deloc}, for fully relaxed disilane, $(ET)_{DS}$, and ethane internal rotation.[26,30] As mentioned and verified in Table 4, the ethane barrier origin can be primarily ascribed to the hyperconjugative effect (ΔE_{deloc}). In particular, this is attributed to vicinal (between methyl) $\sigma_{CH}-\sigma_{CH}^*$ donor−acceptor interactions—reduced in the *syn*-like arrangement of the *E* conformer from that in the *anti*-like arrangement of the *S* conformer (Figure 2a).[1] The exchange effect, $\Delta E_{exchange}$, on the other hand, strongly favors the eclipsed conformation and largely cancels the staggered-conformer-favoring hyperconjugative delocalization energy.[3,9] The structural energy change, favoring the staggered conformer by 2 kcal/mol, is largely attributed to the C−C bond weakening that occurs on torsional rotation (see Section VI).[26] It is smaller than ΔE_{deloc}, but it cannot be neglected in formulating an ethane barrier mechanism.

(b) Hyperconjugation. As expected from the much longer disilane central bond distance, ΔE_{deloc}, the principal barrier forming interaction in ethane, is greatly reduced in disilane—to only 10% of its value in ethane. Comparison of the orbital plots for disilane and ethane in Figure 2 provides a clear explanation. The large separation between σ_{SiH} and σ^*_{SiH} orbitals and unfavorable polarization of the SiH bond (Figure 2b) combine to make the torsional dependency of the overlap between σ_{SiH} and σ^*_{SiH} feeble. In particular, the overlap is only negligibly greater in the favored *anti* arrangement (0.060) over that in the *syn* one (0.056), compared to 0.173 (*anti*) and 0.087 (*syn*) in ethane. If hyperconjugative charge-transfer stabilizations were the sole mechanism controlling the barrier, disilane would exhibit nearly free rotation. From this viewpoint the intriguing question is why is the ∼1 kcal/mol disilane barrier, one-third that of ethane, so large?

In terms of the energy partitioning given in Table 4 two rationalizations can be drawn for the strangely large disilane barrier. The first is reduced magnitude of the antibarrier Pauli exchange interactions, leading to less favoring of the *E* conformer. This decreased exchange effect (compared to ethane) can be viewed as arising from the large separation of the silyl groups. The second reason is that ΔE_{struct}, which encompasses the nonrotational part of the torsional coordinate space, is actually somewhat increased from the 2 kcal/mol value in ethane.

The phantom molecule barrier energetic decomposition, given in Table 4, solidifies this conclusion. ΔE_{deloc} is negligible in the structurally enlarged ethane, $(ET)_{DS}$, showing that attenuation of the hyperconjugative interaction in disilane relative to ethane is almost entirely due to the lengthened central bond in disilane.[31]

(c) Electrostatic Repulsions. The energetic categories discussed above do not explicitly consider electron−electron and nuclear−nuclear repulsions, ΔE_{ee} and ΔE_{nn}. At the outset we note that the steric effect, regardless of whether we are discussing exchange or electrostatic interactions, involves a collective response of the entire N-electron system. It is important to discriminate this simultaneous all-electron effect from local pairwise repulsions obtained by summing independent pair interactions between local bond electron distributions. Figure 3 demonstrates the importance of taking into account the entire space of the torsional coordinate in analyzing electrostatic effects. For pure rotation, i.e., rigid rotation, both electron and nuclear repulsions increase on going to the eclipsed (0°, 120°) conformer. However, when the coordinate space is expanded to include skeletal relaxations (particularly Si−Si bond expansion) as part of the rotational process both repulsions are lowered in going to the eclipsed conformer. The outcome is

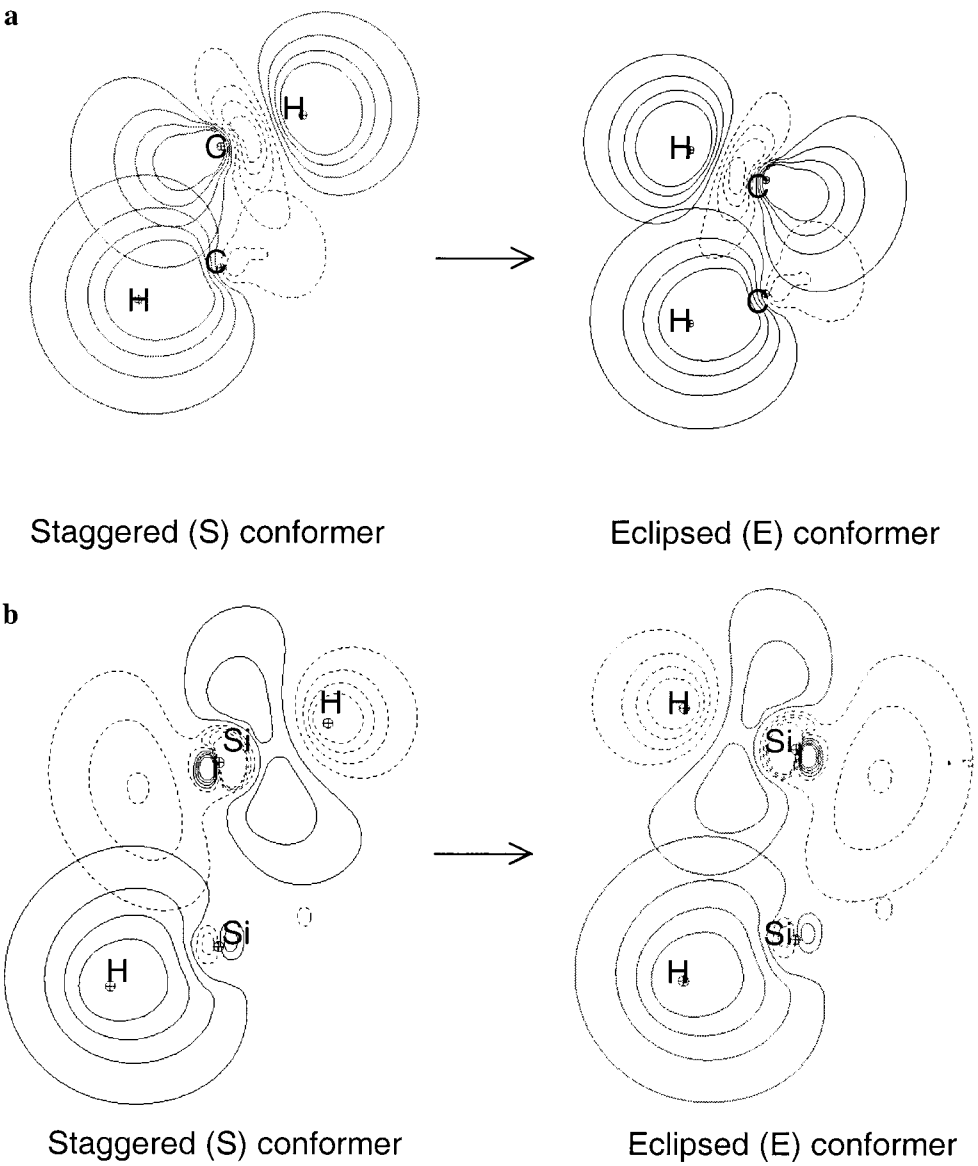

Figure 2. CH/CH* and SiH/SiH* bond/antibond orbital overlaps for the anti (staggered conformer) and syn (eclipsed conformer) arrangements in ethane (a) and disilane (b).

that neither electron nor nuclear repulsions rationalize the disilane barrier.

VI. Flexing Analysis of Disilane Barrier Energy

The electrostatic repulsion analysis described above shows that skeletal relaxation plays a significant role in the rotational energetic mechanism. We turn to nuclear virials to deepen this conclusion. The generalized virial theorem,[32] $T = -E + \lambda$, $2T = -V + \lambda$ relates kinetic (T), potential (V), and total energies (E) to the nuclear virial (λ). The importance of the generalized virial theorem is that it identifies the strain induced effects on T and V. This is because the virial $\lambda = \sum_\alpha \chi_\alpha \cdot F_\alpha$ is the contribution of nucleus α to the virial of the forces acting on the electrons (χ_α is the position vector of nucleus α and $F_\alpha = -\nabla_\alpha V$ is the net force acting on it). When the forces acting on the nuclei vanish (as they must at the variational minimum energy equilibrium conformation (S)), $T_S = -E_S$. A similar result is true for the globally minimized fully relaxed barrier top (E), $T_E = -E_E$. For the conformation reached by disilane rigid rotation, the forces do not vanish and they are repulsive[2] similar to that found for ethane (demonstrated by the large positive values for the increase in the associated nuclear virials for both ethane and disilane in Table 5). Consequently, the molecule is left in a strained state. If only silyl or methyl group relaxation is included in the rotational process (i.e., the Si−Si or C−C bond is frozen) the increase is even larger, but if central bond expansion is included and the silyl/methyl group geometry is frozen (Table 5), the nuclear virial becomes negative. Thus, central bond stretching reduces the strain that is accumulated in both ethane and disilane by rotation alone, instigating a large decrease in electrostatic repulsion energies.

Table 5 shows that the nuclear virial difference (i.e., the strain energy effect) between rigid rotation and the partially relaxed rotation, which includes only central bond expansion, greatly exceeds the $S \rightarrow E$ barrier. This conclusively shows that any explanation for the barrier must take into account the central bond expansion that is inherently a feature of the E conformer geometry.

To explicitly pinpoint the origin of ΔE_{struct} we make use of the flexing diagram shown in Figure 4.[33] The energy increase for each of the diagram steps is given in Table 6. It is clear from the path A energetics (rigid rotation followed by relaxation

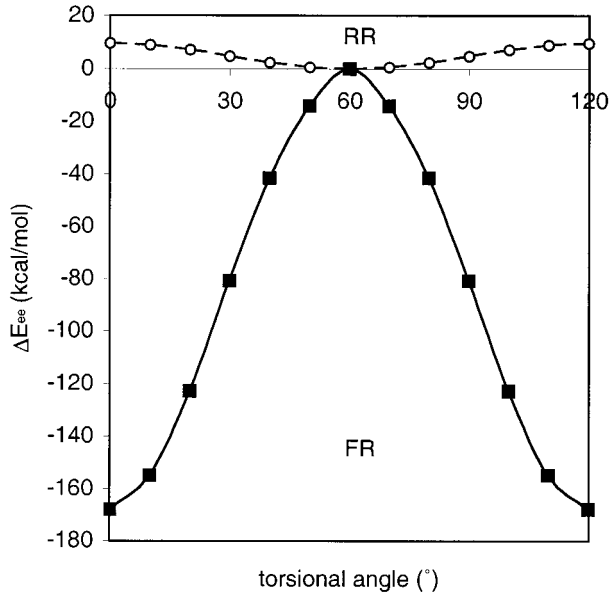

Figure 3. Rotational angle dependence of electron repulsion energy changes for rigid (RR) and fully relaxed (FR) rotations. Corresponding curves for nuclear repulsion have the same trend as the electron ones. 60° denotes the staggered conformer, and 0° and 120° the eclipsed one.

TABLE 5: Nuclear Virials for Disilane and Ethane (kcal/mol)[a,b,c,d]

	disilane	ethane
RR	6.2	12.1
RR + SiH_3 (CH_3) flexing	7.3	16.6
RR + Si−Si (C−C) bond lengthening	−1.7	−4.7
FR	−0.6	−0.2

[a] Disilane, HF/6-311G(3df,2p) geometry optimization and energy calculation; ethane, HF/6-311G(3df,3pd) geometry optimization and energy calculation. Rounded off to the nearest 0.1 kcal/mol. [b] Relative to *S* conformer. [c] Virials are designated by included relaxation(s). RR, rigid rotation. RR+Si−Si (C−C), rotation including Si−Si (C−C in ethane) bond lengthening alone. RR+SiH_3 (CH_3 in ethane), rotation including SiH_3 (CH_3) group flexing alone. FR, fully relaxed rotation, including all skeletal relaxations. [d] The small, but non vanishing value for fully relaxed rotation is due to lack of convergence to the HF limit by the 6-311G(3df,2p) and 6-311G(3df,3pd) basis sets.

of the Si−Si bond) that ΔE_{struct} has its largest contribution from lengthening of the central bond consequent to rotation to the eclipsed conformer.

Path B lengthens the Si−Si bond in the equilibrium staggered conformer followed by rotation. It is clear from the path B energetics that the largest contribution to ΔE_{struct} is again lengthening of the central bond, even though rotation is absent. Hence ΔE_{struct} relates to the Si−Si bond weakening more than to rotation itself. This conclusion that the barrier energetics are significantly determined by non rotational coordinates (i.e., skeletal bond and angle flexings) extending into the torsional coordinate space is parallel to that found for ethane,[10,26] methanol,[34] and propene,[35] but in disilane it becomes paramount.

Given the importance that Si−Si bond expansion has in the barrier mechanism, it is vital to understand what causes the bond lengthening. It is clear from Figure 3 that electrostatic repulsive interactions play a role in the expansion. The effect of hyperconjugation on the expansion can be analyzed by deletion of selected charge-transfer interactions. Following this paradigm, the disilane central bond lengthening is examined through partial geometry optimizations (rotational angle fixed at 60° (*S*) and 0° (*E*)) with selected charge transfers absent. Thus, if shortening

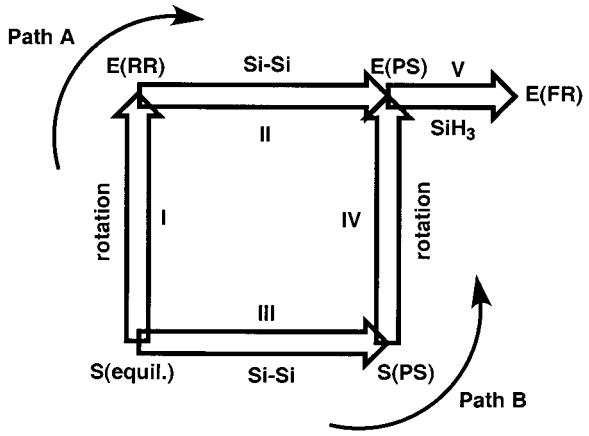

Figure 4. Alternate internal rotation paths to the fully relaxed (FR) eclipsed conformer. In path A (steps I and II), the molecule undergoes rigid rotation (step I), followed by Si−Si bond lengthening (step II). Path B (steps III and IV) relaxes the Si−Si bond length in the staggered equilibrium conformer to its optimized top-of-barrier value (step III), followed by rotation of silyl groups (step IV). Step V additionally relaxes silyl groups to their fully relaxed eclipsed conformer shape.

TABLE 6: Flexing Analysis of Disilane Barrier Energy (kcal/mol)[a,b]

	ΔE_B	ΔE_{struct}	$\Delta E_{exchange}$	ΔE_{deloc}
step I	1.06	1.21	−1.08	0.93
step II	−0.02	1.88	−1.67	−0.23
step III	0.02	1.94	−1.73	−0.17
step IV	1.01	1.15	−1.02	0.88
step V	0.00	−0.13	0.15	−0.02
FR	1.03	2.95	−2.60	0.68

[a] See Table 2, footnote *a*, and Table 4, footnote *b*. [b] For step notation see Figure 4.

of the Si−Si bond accompanies internal rotation upon removal of charge-transfer interactions, hyperconjugation is identified as a factor in its lengthening. On the other hand, if no shortening occurs, hyperconjugative interactions are not a controlling factor for the lengthening. In ethane, we showed that the vicinal hyperconjugation (between methyl groups) is an important factor for the C−C bond lengthening. In disilane, however, the hyperconjugative interactions (Table 6) are greatly weakened from those in ethane, posing the question whether the large Si−Si bond lengthening (0.012 Å) can be accounted for by this mechanism. Upon removal of all possible charge transfers, the central bond undergoes only a small shortening (≤0.003 Å).[36] We conclude that for disilane, unlike for ethane, it is electrostatic repulsive interactions that lead to the bond lengthening.

VII. Conclusions

In terms of the energetic machinery postulated to control the ethane barrier it is the large preferential hyperconjugative interaction in the staggered conformer that is largely responsible for the 3 kcal/mol barrier. Greatly weakened hyperconjugative interactions in disilane rationalize an attenuated barrier, but the 1 kcal/mol barrier magnitude is too high to be accounted for by the residual hyperconjugative stabilization of the equilibrium staggered conformer. We conclude that it is the energetic consequence of the Si−Si bond lengthening that accounts for most of the ∼1 kcal/mol disilane barrier. The major cause for the lengthening is increased electrostatic repulsion in the eclipsed conformer. Instead, in ethane it is the decreased vicinal hyperconjugation in the eclipsed conformer that leads to the C−C bond lengthening.

These results emphasize the role of coordinate space in understanding barrier energetics. Even though ethane and disilane exhibit similar central bond expansions, in ethane the effect of C−C bond weakening is overwhelmed by the large, rotationally controlled change in hyperconjugative interactions. In disilane, however, weakened hyperconjugative interactions leave the nonrotational part of the torsional coordinate as the paramount contribution to the barrier energetics.

In summary, the same gears and motors that operate in the ethane barrier are found to operate in a different way for disilane.

Acknowledgment. Financial support from NSF and computational support from the San Diego Supercomputer Center are gratefully acknowledged.

References and Notes

(1) Reed, A. E.; Weinhold, F. *Isr. J. Chem.* **1991**, *31*, 277−285.
(2) Bader, R. F. W.; Cheeseman, J. R.; Laidig, K. E.; Wiberg, K. B.; Breneman, C. *J. Am. Chem. Soc.* **1990**, *112*, 6530−6536.
(3) Goodman, L.; Pophristic, V.; Weinhold, F. *Acc. Chem. Res.* **1999**, *32*, 983−993.
(4) Sovers, O. J.; Kern, C. W.; Pitzer, R. M.; Karplus, M. *J. Chem. Phys.* **1968**, *49*, 2592−2599.
(5) Pitzer, R. M. *Acc. Chem. Res.* **1983**, *16*, 207−210, and references therein.
(6) Christiansen, P. A.; Palke, W. E. *Chem. Phys. Lett.* **1975**, *31*, 462−466.
(7) Brunck, T. K.; Weinhold, F. *J. Am. Chem. Soc.* **1979**, *101*, 1700−1709.
(8) England, W.; Gordon, M. S. *J. Am. Chem. Soc.* **1971**, *93*, 4649−4657.
(9) Badenhoop, J. K.; Weinhold, F. *Int. J. Quantum Chem.* **1999**, *72*, 269−280.
(10) Pophristic, V.; Goodman, L. *Nature* **2001**, *411*, 565−568.
(11) Beagley, B.; Conrad, A. R.; Freeman, J. M.; Monaghan, J. J.; Norton, B. G.; Holywell, G. C. *J. Mol. Struct.* **1972**, *11*, 371−380.
(12) Cho, S. G.; Rim, O. K.; Park, G. *J. Comput. Chem.* **1997**, *18*, 1523−1533, and references therein.
(13) Durig, J. R.; Church, J. S. *J. Chem. Phys.* **1980**, *73*, 4784−4797.
(14) Chattaraj, P. K.; Nath, S.; Sannigrahi, A. B. *J. Phys. Chem.* **1994**, *98*, 9143−9145.
(15) Schleyer, P. v. R.; Kaupp, M.; Hampel, F.; Bremer, M.; Mislow, K. *J. Am. Chem. Soc.* **1992**, *114*, 6791−6797.
(16) Scott, R. A.; Scheraga, H. A. *J. Chem. Phys.* **1965**, *42*, 2209−2215.
(17) Profeta, S., Jr.; Unwalla, R. J.; Cartledge, F. K. *J. Comput. Chem.* **1989**, *10*, 99−103.
(18) Topiol, S.; Ratner, M. A.; Moskowitz, J. W. *Chem. Phys.* **1977**, *20*, 1−17.
(19) Nicolas, G.; Barthelat, J. C.; Durand, P. *J. Am. Chem. Soc.* **1976**, *98*, 1356−1350.
(20) Gordon, M. S.; Neubauer, L. *J. Am. Chem. Soc.* **1974**, *96*, 5690−5693.
(21) Hinchliffe, A. *J. Mol. Struct.* **1978**, *48*, 279−283.
(22) Leszczynski, J.; Huang, J. Q.; Schreiner, P. R.; Vacek, G.; Kapp, J.; Schleyer, P. v. R.; Scheafer, H. F., III. *Chem. Phys. Lett.* **1995**, *244*, 252−257.
(23) Frisch, M. J.; Trucks, G. H.; Schlegel, H. B.; Scuseria, G. E.; Rob, M. A.; Cheeseman, J. R.; Zakrzewski, V. G.; Montgomery, J. A.; Stratmann, R. E.; Burant, J. C.; Dapprich, S.; Millam, J. M.; Daniels, A. D.; Kudin, K. N.; Strain, M. C.; Farkas, O.; Tomasi, J.; Barone, V.; Coss, M.; Cammi, R.; Mennucci, B.; Pomelli, C.; Adamo, C.; Clifford, S.; Ochtersk, J.; Petersson, G. A.; Ayala, P. Y.; Cui, Q.; Morokuma, K.; Malick, D. K.; Rabuck, A. D.; Raghavachari, K.; Foresman, J. B.; Cioslowski, J.; Ortiz, J. V.; Stefanov, B. B.; Liu, G.; Liashenko, A.; Piskorz, P.; Komaromi, I.; Gomperts, R.; Martin, R. L.; Fox, D. J.; Keith, T.; Al-Laham, M. A.; Peng, C. Y.; Nanayakkara, A.; Gonzalez, C.; Challacombe, M.; Gill, P. M. W.; Johnson, B. G.; Chen, W.; Wong, M. W.; Andres, J. L.; Head-Gordon, M.; Replogle, E. S.; Pople, J. A. *Gaussian 98*; Gaussian, Inc.: Pittsburgh, PA, 1998.
(24) Glendening, E. D.; Badenhoop, J. K.; Reed, A. E.; Carpenter, J. E.; Weinhold, F. NBO 4.M.; Theoretical Chemistry Institute, University of Wisconsin, Madison, 1999.
(25) Weinhold, F. Natural Bond Orbital Methods. In *The Encyclopedia of Computational Chemistry*; Schleyer, P. v. R., Allinger, N. L., Clark, T., Gasteiger, J., Kollman, P. A., Schaefer, H. F., III, Schreiner, P. R., Eds.; John Wiley & Sons: Chichester, 1998; Vol. 3; pp 1792−1811.
(26) Goodman, L.; Gu, H.; Pophristic, V. *J. Chem. Phys.* **1999**, *110*, 4268−4275.
(27) Reed, A. E.; Curtiss, L. A.; Weinhold, F. *Chem. Rev.* **1988**, *88*, 899−926.
(28) Steric repulsions, as understood by the bulk of organic chemists comprise the sum of two repulsive interactions: the short-range Pauli exchange repulsions (a quantum mechanical effect) and the simple Coulomb repulsions between like charges (a classical $1/R$ effect).
(29) Badenhoop, J. K.; Weinhold, F. *J. Chem. Phys.* **1997**, *107*, 5406−5421.
(30) Studies on the influence of relaxation on the antisymmetrization effect (ref 33) show that $\Delta E_{\text{exchange}}$ is strongly dependent on geometry details. If idealized unrelaxed geometries are used to describe internal rotation in ethane, the rotation effect on exchange energy is much smaller than ΔE_{deloc}, but when optimized ethane geometries are employed, it is large and comparable to ΔE_{deloc}.
(31) It is interesting to note that the electron enriched ethane $(DS)_{ET}$ eclipsed preferred structure can be understood in this approach by the large increase in the magnitude of the eclipsed conformer favoring exchange interaction, $\Delta E_{\text{exchange}}$, compared to its value in ethane (22 vs 6 kcal/mol). Since ΔE_{struct} also favors the eclipsed structure, these interactions overwhelm the staggered structure favoring hyperconjugative interaction.
(32) Slater, J. C. *J. Chem. Phys.* **1933**, *1*, 687−691.
(33) Goodman, L.; Gu, H. *J. Chem. Phys.* **1998**, *109*, 72−78.
(34) Pophristic, V.; Goodman, L. *J. Am. Chem. Soc.*, submitted.
(35) Goodman, L.; Leszczynski, J.; Kundu, T. *J. Am. Chem. Soc.* **1993**, *115*, 11991−11996.
(36) Calculated shortening for various basis sets ranges from 0.002 Å (double-ζ family) to 0.003 Å (triple-ζ family).